Study on the Durability of Industrial Waste-MgO Synergistically Cured Silty Sand under Dry and Wet Cycle Conditions

Zhaochang Zhang*, Qiang Wang
School of Civil Engineering and Architecture, Anhui University of Science and Technology, Huainan, Anhui, China
**Corresponding Author.*

Abstract: Aiming at the common problems of low utilization of industrial solid waste and insufficient performance of pulverized sandy soil roadbase, this study investigated the effect of dry and wet cycles on the mechanical properties of slag-target slag-MgO synergistically cured pulverized sandy soil. The study investigates the impact of dry and wet cycles on the mechanical properties of cured silt soil using unconfined compressive strength tests, mass loss rate measurements, and microscopic characterization techniques such as X-ray diffraction (XRD) and scanning electron microscopy (SEM). It analyzes the changes in hydration products, the bonding strength between soil particles, and the microstructural variations. The results of the study showed that: As the number of wet and dry cycles increased, the mass loss rate of the specimens varied between 14.95% and 18.88%. The strength exhibited a pattern of rising and then falling, with a peak value of 3.90 MPa. the microstructure analysis showed that, with the increase of the number of cycles, the mineral composition of cured silt loam changed, the quartz diffraction peaks were weakened, and the diffraction peaks of the hydration products (e.g., AFt, M-S-H, C-A-H) were enhanced, forming a more compact structure, and improving the structure of cured silty sand, forming a more compact structure and enhancing the strength of the soil. The hydration products of the specimens with high hardener dosage fill the pores, enhance the particle bonding and show higher compressive strength, while the specimens with low hardener dosage have more pores and lower strength due to incomplete hydration reaction or structural damage. The research results can provide theoretical support for the research and development of environmentally friendly slag - calcium carbide slag - MgO cementitious materials and their application in the field of soil reinforcement, such as curing of silty sand

Keywords: Consolidation of Silty Sand; Wet and Dry Cycles; Unconfined Compressive Strength; Microscopic Properties

1. Introduction

As urban modernization in China progresses rapidly, the construction of transportation infrastructure requires more and more performance of geotechnical engineering materials. As a key part of road engineering roadbed soil, its mechanical properties and stability directly determine the service life of the pavement. It is worth noting that China's vast territory, North China, Northwest China and other regions are commonly distributed in the silt sand soil, but silt sand soil has the characteristics of poor particle grading, low plasticity index, etc., and there are usually problems such as difficult to meet the standard of compaction, insufficient compressive strength and so on, which also greatly limits its use as a roadbed filler [1]. Especially in monsoon climate zones, seasonal dry and wet alternation makes such soils susceptible to moisture, therefore, it is necessary to use curing materials to improve the silt sandy soil in order to improve the stability and bearing capacity of its filled roadbase. Although the traditional lime curing treatment can improve the soil, the strength of the soil may decrease by more than 40% after 10 dry and wet cycles [2]. How to improve the performance deficiencies of traditional curing technology and develop new soil curing agent systems adapted to complex environments has become an urgent technical challenge in the field of

geotechnical engineering.

Industrial wastes have a long history of use, among which wastes such as steel slag, fly ash, and slag have been widely used in soil improvement studies due to their strong chemical activity. Many studies have shown that the addition of steel slag, fly ash and other waste materials can effectively increase the compressive strength of the soil, and also improve the resistance of the soil to dry and wet changes and erosion. These waste slag materials participate in hydration reactions in the soil to produce compounds that fill the pores between the soil thus giving it a dense structure. In particular, steel slag is rich in calcium oxide (CaO), which reacts with water to produce hydrated calcium hydroxide ($Ca(OH)_2$), thus effectively improving the compressive strength of the soil [3]. However, there are some problems associated with the simple use of industrial wastes to improve soil, such as slow hydration rate, insufficient stability, and poor adaptability to the environment. In order to overcome these problems, magnesium oxide (MgO), as a low-carbon and environmentally friendly soil curing agent, has gradually gained attention in recent years [4]. During the hydration process, magnesium oxide produces hydrated magnesium oxide ($Mg(OH)_2$), a reaction that enhances the strength, stability, and durability of the soil. [5-6]. It has been shown that MgO not only enhances the compressive strength of soil in the short term, but also further enhances the mechanical properties of the soil body in the long-term hydration process. Despite the outstanding effect of MgO in curing soil, its effect may be limited due to its slow hydration reaction, especially under complex environmental conditions such as dry and wet cycles. Therefore, how to find a good combination of industrial wastes and MgO through synergistic effects to improve the durability of soil under dry and wet cycling conditions has become a key important topic in the current research on soil curing agents [7-8].

The dry-wet cycle, used as an experimental method to mimic natural environmental changes, can highlight how repeated wetting and drying affect the physical and mechanical properties of the soil, particularly its pore structure.[9]. Under the action of wet and dry cycles, the repeated adsorption and evaporation of water in the soil leads to changes in its physical properties such as porosity and dry density, which in turn affects the strength and stability of the soil. The effect of dry and wet cycles is especially obvious for soils with poor water retention capacity such as silt soils. Therefore, studying the durability of industrial waste and MgO synergistically cured silt loam under dry and wet cycling conditions not only helps to improve the mechanical properties of the soil, but also further improves its adaptability under special environments. Existing studies have shown that the mechanical properties and resistance to environmental changes of soil can be significantly enhanced by adding industrial waste slag with strong alkalinity (e.g., steel slag, calcium carbide slag) synergistically cured with MgO [10]. Under certain conditions, the strength of MgO-slag modified soil can reach three times of the strength of cemented soil, and the content of unstable products such as hydrated calcium silicate-aluminate (C-A-S-H) as well as calcovanadate (AFt) in MgO-slag modified soil is much lower than that of cemented soil, which makes the MgO-slag modified soil possess better stability and erosion resistance [11]. This synergistic effect not only accelerates the hydration reaction, but also effectively reduces the negative impact of moisture changes on soil properties. However, the existing studies on the synergistic curing of soil with industrial slag and MgO under dry and wet cycling conditions are fewer, which is not conducive to practical engineering applications.

This paper aims to further investigate the durability of silt soil cured with a new agent made from slag, MgO, and calcium carbide slag under dry and wet cycling conditions. The study examines the mechanical and microscopic properties during the dry-wet cycles using unconfined compressive strength tests, X-ray diffraction, and scanning electron microscopy. The goal is to explore a new approach for reusing industrial curing wastes while also offering technical support for the practical application of cured silt soil in real-world projects. At the same time, it provides technical support for the application of cured powdered sandy soil in practical engineering.

2. Materials and Methods

2.1 Test Material

The test soil samples were taken from Pingxu, Panji District, Huainan City, and the color was gray-black and fluid-plastic state. After drying and airing, the color became lighter and was in the state of sandy soil. Its sand content was 62.3%. According to the Standard of Soil Engineering Classification GB/T 50145-2007, the soil sample belongs to sandy soil, with 37.7% of fine-grained soil content and more than 50% of powdered grains, which is called pulverized sand (code SM). Adopting the Standard for Geotechnical Test Methods (GB/T50123-2019), the physical and mechanical parameters of this chalky sandy soil measured by the test are shown in Table 1.

Table 1. Basic Physical Indicators of Silt

Moisture content range/%	relative density	liquid limit/%	plastic limit/%	plasticity index
37-52	2.46	25.2	18.6	6.6

The main chemical and mineral compositions of slag, calcium carbide slag and MgO used in the test are shown in Table 2. It can be found that the total amount of CaO, MgO, SiO_2 and Al_2O_3 in the slag is as high as 89.66%, and the main mineral compositions are calcium silicate ($CaSiO_3$), calcium-aluminum silicate ($Ca_2Al_2SiO_7$), and $CaCO_3$, etc.; and the main composition of calcium carbide slag is $Ca(OH)_2$.

Table 2. Curing Agent Material Composition

curing agent	SiO_2	Al_2O_3	Fe_2O_3	CaO	MgO	SO_3	Na_2O
slag	35.22	20.16	1.42	28.31	5.97	1.46	0.12
calcium carbide slag	2.47	2.16	0.24	69.82	0.13	0.85	0.04
MgO	2.65	0.20	0.20	1.60	93.57	—	—

2.2 Experimental Methods

In this experiment, based on the previous experiments, the unconfined compressive strength (UCS) was used as an index, and the best curing agent ratio was when the proportion of slag (GGBS): MgO: calcium carbide slag (CCR) admixture was 15:8:7, so the ratio was adopted to study the durability performance of cured silt soil, and the curing agent admixture of this experiment was designed as 25%, 30% and 35% (ratio of the mass of curing agent to the mass of silt soil) Abbreviated as S25, S30, S35 respectively.

Firstly, the curing process is carried out on the chalky sandy soil according to the designed curing agent dosage. After preparation, the specimens are subjected to a standard maintenance period of 28 days to ensure that the curing process achieves the desired results. After the curing period, the specimens were labeled and marked to facilitate the subsequent recording of experimental data. Subsequently, three groups of specimens with different dosages were subjected to wet and dry cycle tests to investigate the influence of wet and dry cycles on the quality and strength of cured silty sand

The wet and dry cycle test is set up as a 12-stage cycle with 0w, 1w, 2w, 3w, 4w, 5w, 6w, 7w, 8w, 9w, 10w, 11w, and 12w. Where each stage of the wet and dry cycle consists of two steps, the wet cycle and the dry cycle. In the wet cycle stage, the specimen will be immersed in water for 12 hours; in the dry cycle stage, the specimen needs to be dried at a constant temperature of 35°C for 11 hours. Finally, the specimens are allowed to stand at room temperature for 1 hour to complete a full cycle. Strength tests were performed on the specimens after completing the designated cycles to evaluate the changes resulting from different numbers of wet and dry cycles. By comparing the mass change and strength data of the specimens under different cycle times and different curing agent dosages, the effect of wet and dry cycles on the mass, strength and structural properties of cured silt loam was revealed.

3. Analysis of Test Results

3.1 Influence of Dry and Wet Cyclic Action on the Quality of Cured Chalky Soils

After 28 days of curing, the cured powdered sandy soil specimens were subjected to wet and dry cycling tests in order to investigate the effect of wet and dry cycling on the quality change and strength of the specimens. Each level of cycling consisted of two main phases, namely the soaking phase and the drying phase.

The first step of the test was to accurately weigh the initial mass (M_0) of each specimen

block using an electronic scale and record this data. Next, the specimens were wetted by placing them in a tank of water to ensure that they were completely submerged. The immersion process lasted for 12 hours to fully simulate the wetting conditions. At the end of the water immersion, the surface of the specimen was gently wiped with a clean, dry towel to remove excess water from the surface in order to avoid moisture interference with the mass measurement. At this point, the wet mass (M_w), which represents the mass of the specimen in the wet condition, was immediately weighed and recorded using an electronic scale.

Next, the specimens were subjected to a drying phase. The specimens are placed in a drying environment in an oven at a constant temperature of 35°C for 11 hours. During the drying process, the moisture of the specimens gradually evaporates and changes in quality occur. Immediately after the end of drying, the specimens were removed from the oven and weighed again with an electronic scale to obtain the dry mass (M_d), which reflects the mass of the specimens in the dried state.

Through these steps, the mass data at each cycle stage can be obtained and the rate of mass change (Δm) and cumulative dry mass loss (C_i) for different number of wet and dry cycles (n) are calculated according to the following equations (1) and (2). And they were plotted in Figures 1 and 2.

The rate of mass change is calculated as:

$$\Delta m_n = \frac{M\omega_n - M_0}{M_0} \times 100\% \quad (1)$$

where Δm_n denotes the rate of mass change of the specimen after the nth cycle, Mwn is the wet mass of the specimen after the nth wet cycle, and M0 is the initial mass.

The cumulative dry mass loss rate is calculated as:

$$C_i = \frac{M_0 - M_{di}}{M_0} \times 100\% \quad (2)$$

where C_i denotes the cumulative dry mass loss rate after the ith wet/dry cycle, Mdi is the dry mass of the specimen after the ith cycle, and M_0 is the initial mass of the specimen.

Figure 1 illustrates the relationship between the mass change rate of cured silt soil specimens and the number of dry-wet cycles. In general, the mass change rate of the specimens remains relatively low, ranging from -3.132% to 1.691%. This phenomenon indicates that the quality change of cured siltstone is relatively stable under the action of several dry and wet cycles. The reason for this is that the poor water retention of the silt sand soil itself leads to its limited water absorption capacity and poor water retention. In particular, compared to other soil types, silt loam loses water faster in the wet state, which keeps the magnitude of its mass change within a relatively small range during the wet and dry cycles.

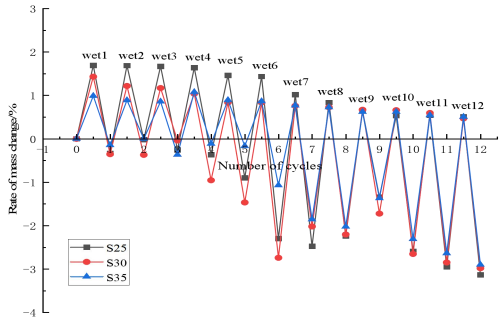

Figure 1. The Relationship between the Number of Cycles and the Mass Change Rate

The mass changes of the three specimen groups (S25, S30, and S35) with varying doping amounts followed a similar pattern. Initially, after the first wet cycle stage, the overall mass of the specimens increased. This was because water entered the pores of the silt loam during the wet cycle, leading to an increase in mass. The rate of change in mass for specimens S25, S30, and S35 were 2.45%, 2.00%, and 1.41%, respectively. However, this trend of mass increase would not be maintained. In the subsequent wet cycles, the magnitude of the mass change of the test blocks gradually decreased, especially at the end of the twelfth level of wet cycle, the rate of mass change of the test blocks S25, S30, and S35 decreased to 0.51%, 0.57%, and 0.51%, respectively. This trend suggests that as the number of wet cycles increases, the water absorption capacity of the cured siltstone soil decreases. This may indicate that the soil's pore structure approached saturation during the repeated wetting process, leading to a reduced impact of subsequent wet cycles on mass changes.

In the dry cycle stage, the situation was different from the wet cycle. At the end of the first stage of dry cycling, the quality of all the

specimens showed an overall decreasing trend, and the rate of change in the quality of specimens S25, S30, and S35 was 0.33%, -0.36%, and -0.15%, respectively. In this stage, the water inside the cured silt soil gradually evaporated due to the dry cycling effect, which led to the decrease in its quality. Especially in the first five stages of dry cycling, the mass loss of the three groups of specimens was relatively small (0.02% to 0.95%). This indicates that in the initial dry cycling stage, the evaporation of water is slower and the quality change of the specimens is smoother.

In summary, the cured silt sand specimens showed a certain pattern of quality change in the process of wet and dry cycles, the wet cycle stage mainly affects the absorption of water and pore filling, while the dry cycle changes the pore structure through water evaporation, which leads to a more obvious quality loss. The difference in the quality of the specimens with different dosage is due to the porosity, unreacted material content and the different absorption capacity of water.

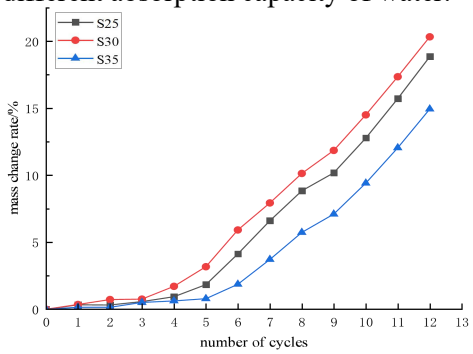

Figure 2. Cumulative Mass Loss Rate at Different Number of Cycles

Figure 2 presents the relationship curves between the number of dry-wet cycles and the cumulative mass loss rate of the cured silt soil specimens. As the wet and dry cycles progressed, the cumulative mass loss rates of specimens S25, S30, and S35 exhibited a similar increasing trend. With the rise in the number of cycles, the mass loss rate steadily increased, and the rate of growth accelerated over time. This trend indicates that the repeated action of wet and dry cycles has a continuous effect on the quality of the specimens, leading to different degrees of quality loss in different specimen blocks after several wet and dry cycles. Comparing the cumulative mass loss rates of the three specimen groups reveals that specimen S35 had the lowest rate, followed by S25, while S30 exhibited the highest cumulative mass loss rate.

As the number of wet and dry cycles increased, the specimens underwent repeated water absorption and evaporation, leading to changes in the moisture content and significant damage to their internal structure. The repeated cycles gradually weakened the cementation between soil particles, causing a decline in the strength of particle bonds. This led to the formation of larger internal pores and more cracks. On a larger scale, these changes were reflected in the shedding of soil particles from the specimen surface, ultimately resulting in a higher cumulative mass loss rate and an accelerated increase in this rate.

After 12 levels of wet and dry cycling, the cumulative mass loss of test blocks S25, S30, and S35 were 18.88%, 20.34%, and 14.95%, respectively. These data indicate that there are some differences in the wet and dry cycling resistance of the test blocks with different curing agent dosages. Overall, specimen block S35 showed the best dry and wet cycling durability performance with the lowest cumulative mass loss rate, which indicates that its structural damage under dry and wet cycling is less severe and has stronger stability. On the other hand, the cumulative mass loss rate of test block S30 was higher, indicating its weaker resistance to dry and wet cycling.

3.2 Effect of Number of Wet and Dry Cycles on Strength

Figure 3 illustrates the relationship between the number of dry-wet cycles and the compressive strength of the cured silt sand specimens. Under the wet and dry cycling conditions, the unconfined compressive strength of all three specimen groups initially increased and then decreased as the number of cycles increased. At the start of the cycle, the unconfined compressive strength of the specimens saw a notable increase after the second wet and dry cycle. For specimen S25, the strength rose from 2.01 MPa to 2.41 MPa, reflecting a growth of 19.9%. Specimen S30's strength increased from 2.88 MPa to 3.00 MPa, a 4.2% rise, while specimen S35 saw its strength grow from 3.40 MPa to 3.90 MPa, a 14.71% increase. This change may be due to the fact that the internal hydration reaction is still going on in the specimen after 28 days of standard curing, and the moisture in the

wet-cycle process provides more reactants for the hydration reaction, which promotes the reaction to be more complete, thus the strength of the specimen is improved.

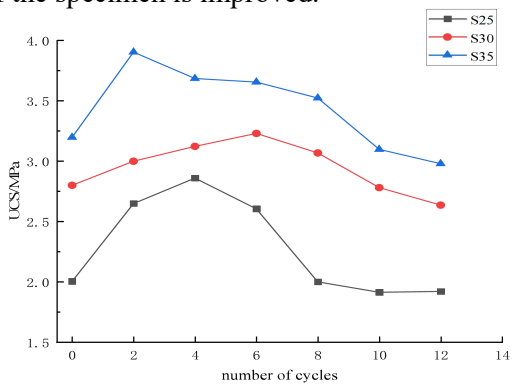

Figure 3. The Relationship between the Number of Cycles and Strength

However, as the number of wet and dry cycles continued to increase, the compressive strength of the specimens began to decrease. After the 4th wet/dry cycle, the compressive strength of specimen S35 dropped from 3.90 MPa to 3.69 MPa. Specimen S25 experienced a decrease in strength from 2.60 MPa to 2.37 MPa after the 6th cycle, while specimen S30's strength reduced from 3.33 MPa to 3.07 MPa following the 8th cycle. The change was due to the fact that the hydration products inside the specimen would change in the process of repeated wetting and drying during the wet/dry cycle, resulting in the internal structure of the specimen. This change is due to the fact that during wet-dry cycling, the hydration products inside the specimen block will change during repeated wetting and drying, which leads to the appearance of pores in the internal structure of the specimen. As the number of wet and dry cycles increases, these pores progressively enlarge, causing damage to the specimen's internal structure. This results in a visible reduction in compressive strength.

After 12 wet and dry cycles, the compressive strength of silt loam cured with different amounts of curing agent showed varying degrees of reduction. Specimen S25's compressive strength dropped from 2.01 MPa to 1.75 MPa, a decrease of 12.9%; specimen S30's compressive strength reduced from 2.88 MPa to 2.64 MPa, a loss of 8.3%; and specimen S35's compressive strength fell from 3.20 MPa to 2.98 MPa, representing a decrease of 6.8%. This pattern indicates that the cured powdered sandy soil specimens demonstrate good resistance to wet and dry cycles. As the curing agent dosage increases, the compressive strength decreases less, with the S35 samples showing the smallest loss and the best durability.

4. Microscopic Properties of Cured Silt Loam under Dry and Wet Action

4.1 XRD Results Analysis

XRD test can effectively detect the physical phase in cured silt soil and analyze the mineral composition in it in detail. In order to investigate the effect of wet and dry cycling on the mineral composition of cured silt loam, specimen block S30 was selected in this study for different numbers of wet and dry cycling, which were noted as S30W0 (0-stage cycling), S30W6 (6-stage cycling), and S30W12 (12-stage cycling), respectively. These specimen blocks were subjected to wet and dry cycling and will be further analyzed in terms of microstructure to explore the effect of the cycling process on the mineral composition and structural changes of the specimens.

Figure 4 presents the X-ray diffraction (XRD) analysis results for the specimen blocks S30W0, S30W6, and S30W12. The comparison shows a gradual reduction in the intensity of the quartz diffraction peaks as the number of wet and dry cycles increases. This indicates that the mineral composition of the cured siltstone soil has experienced notable changes after several wet and dry cycles, particularly with ongoing hydration reactions that lead to the transformation of certain minerals or further interaction with water.

Specifically, the diffraction peak of quartz is most obvious in specimen block S30W0, indicating that the quartz mineral content in this specimen is high and the hydration reaction has not yet been fully carried out. With the increase in the number of wet and dry cycles, the intensity of quartz diffraction peaks in block S30W6 decreased, indicating that part of the quartz minerals had participated in the hydration reaction and transformed into other hydration products. In S30W12, the intensity of quartz diffraction peaks was further weakened, indicating that the hydration reaction had been more complete and the mineral composition of the soil body had changed significantly. However, as the number of wet and dry cycles increased, the specimen's internal structure was damaged, leading to the

gradual deterioration of the soil skeleton. This caused an increase in pore space, resulting in a decrease in strength and a more chaotic XRD pattern. Additionally, the intensity of the $Ca(OH)_2$ diffraction peak gradually diminished, further confirming that the specimen's alkalinity decreased with the increasing number of cycles, indicating a progressive deepening of the hydration reaction.

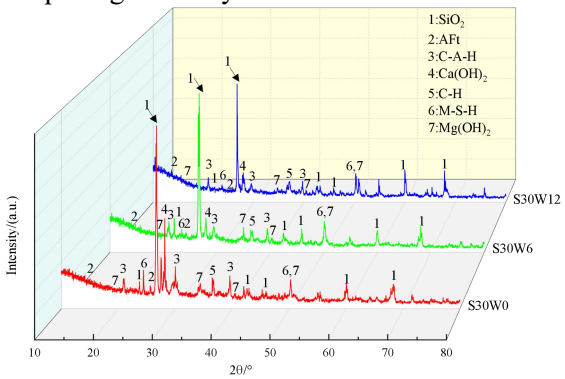

Figure 4. XRD Diffraction Patterns of Solidified Silty Soil under Different Stages of Wet-dry Cycles

In test block S30W6, the diffraction peak intensities of the hydration products such as AFt, M-S-H and C-A-H reached the highest values, and these hydration products helped to fill the pores between the particles, which further enhanced the compressive strength of the soil. Macroscopically, the compressive strength of specimen S30W6 was higher than the other two specimens. Taken together, the dry and wet cycles affected the mineral composition and mechanical properties of the cured silt loam, and the further occurrence of hydration reactions played a key role in enhancing the strength of the soil.

4.2 SEM Results Analysis

Scanning electron microscope (SEM) tests were performed on three sets of specimens, S30W0, S30W6 and S30W12. A magnification of 500 times was chosen to fully examine the appearance characteristics of the cured silt soil samples, and a magnification of 2000 times was used to observe the internal product changes of the cured silt soil. The test results are shown in Figure 5 below.

In the 500x magnified image, the irregular granular structure is clearly demonstrated, with close contact between the particles, forming a dense structure after curing action. The amorphous C-A-H gel hydration products are distributed on the surface of the particles and in their interstices, and these hydration products enhance the connection between the soil particles and show better structural stability. Comparing images (a), (c) and (e), it can be seen that the internal structure of block S30W6 is the most compact, with hydration products filling almost all the pores, showing good overall compactness and macroscopically high compressive strength, while blocks S30W0 and S30W12 are more porous and have weaker bonding between soil particles. The weak bonding of S30W0 is due to incomplete hydration reaction, while that of S30W12 is due to multiple drying. The weak bonding of S30W0 is due to incomplete hydration reaction, while the internal structure of S30W12 is damaged due to multiple wet and dry cycles.

In the 5000× magnification images, the analysis of specimen blocks S30W0, S30W6, and S30W12 showed that the rose-like M-S-H and C-S-H hydration products interacted to form agglomerates, and these agglomerates not only bonded the soil particles, but also filled the pore spaces, which enhanced the strength of the soil body. By comparing images (b), (d), and (f), it is evident that the number of pores within the soil body initially increases and then decreases as the wet and dry cycles progress. Additionally, the image of S30W12 displays the loosest structure. Concurrently, the quantity of hydration products increases over time, forming larger agglomerates and creating a denser mesh-like structure.

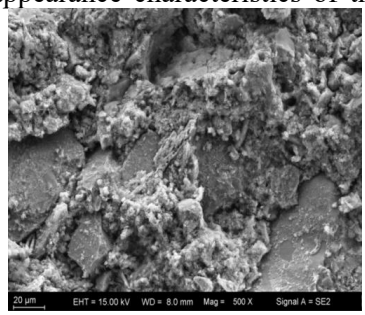

(a) S30W0(×500)

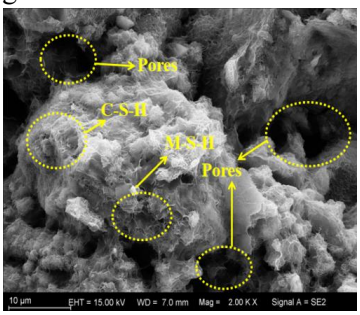

(b) S30W0(×2000)

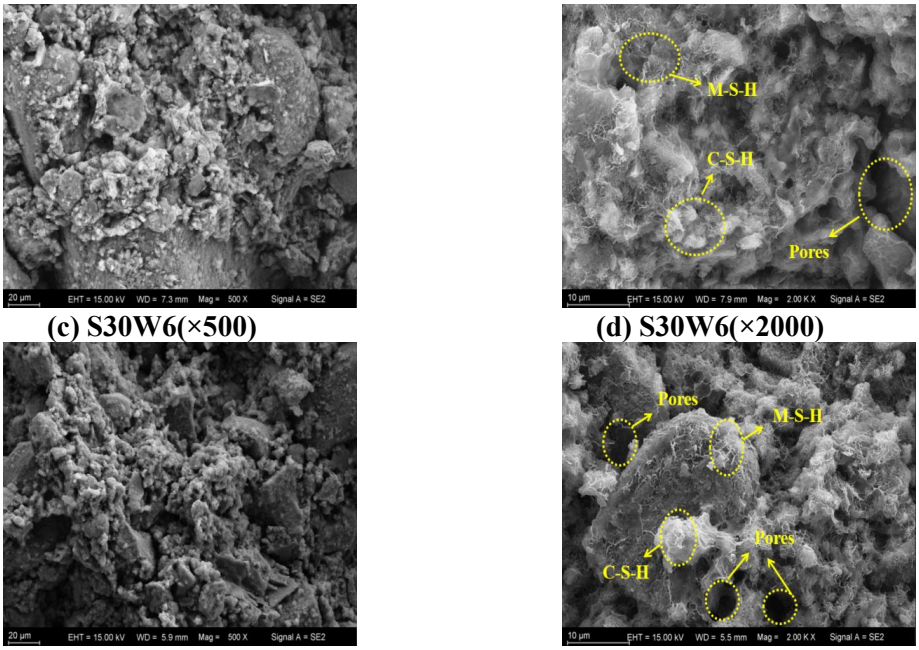

(c) S30W6(×500) (d) S30W6(×2000)

(e) S30W12(×500) (f) S30W12(×2000)

Figure 5. SEM Patterns of Solidified Silty Soil under Different Stages of Dry-wet cycles

5. Conclusions

This chapter takes slag, calcium carbide slag and MgO cured silt as the research object, according to the ratio of slag: MgO: calcium carbide slag = 15:8:7 set up three groups of test blocks with different curing agent dosage, the main study is the number of dry and wet cycles on the quality change of silt specimens, mechanical properties of the influence of the law, combined with the microscopic test to analyze the changes in the internal products and structure of cured silt under the conditions of dry and wet cycles, and obtain the following conclusions The following conclusions are obtained:

1. As the duration of the wet and dry cycles increased, both the rate of mass change and the cumulative mass loss rate of the specimens decreased. After 12 cycles, the cumulative mass loss rates for specimens S25, S30, and S35 were 18.875%, 20.341%, and 14.950%, respectively, suggesting that the cured siltstone soil exhibits strong resistance to dry and wet cycles.

2. With the progression of wet and dry cycles, the unconfined compressive strength of the cured silt sand specimens initially increased before gradually decreasing. After 12 cycles, the compressive strength of specimen S25 reduced from 2.01 MPa to 1.75 MPa, while specimen S30 saw a decrease from 2.88 MPa to 2.64 MPa, and specimen S35 dropped from 3.20 MPa to 2.98 MPa. This trend highlights the complex behavior of the specimens under repeated wet and dry conditions, with an initial improvement followed by a decline in strength.

3. The XRD and SEM results of microscopic tests show that: with the increase of the number of wet and dry cycles, the mineral components of the cured siltstone soil changed significantly, the intensity of the quartz diffraction peaks gradually weakened, the hydration reaction advanced leading to the transformation of the minerals, and the hydration products, such as the diffraction peaks of AFt, M-S-H, and C-A-H were enhanced, which strengthened the strength of the soil body, especially in the S30W6 specimen; the hydration products gradually strengthened under the wet and dry cycles, forming a compact structure, especially in the S30W6 specimen; and the S30W6 specimen showed high compressive strength. Under the dry and wet cycles, the hydration products gradually enhanced and formed a compact structure, especially in the S30W6 specimen, the hydration products filled the pores and enhanced the bonding force of the soil particles, which showed high compressive strength; while S30W0 and S30W12 had more pores and lower strength due to the incomplete hydration reaction or structural damage caused by multiple cycles.

References

[1] Zhang Y.L, Zhou L.G., Wang J, et al. Effect of freezing and thawing on mechanical properties of chalky sandy soil and stability of embankment slopes. Journal of Jilin University (Engineering Edition),2019, 49 (05): 1531-1538.

[2] Huang Hu, Song C.B., Gao Y., et al. Research on microscopic permeability mechanism of lime-amended sandy soil. Hydropower Energy Science, 2024, 42(12):101-105.DOI:10.20040/j.cnki.1000-7709.2024.20241659.

[3] Shi Y., Wang X. Research on the preparation and properties of steel slag-dredged silt mixed cured soil. Green Building Materials, 2020, (11): 8-9. DOI:10.16767/j.cnki.10-1213/tu.2020.011.004.

[4] YI Y, GU L, LIU S, et al. Magnesia reactivity on activating efficacy for ground granulated blastfurnace slag for soft clay stabilization. Applied Clay Science, 2016, 126: 57-62.

[5] Wang D.X., He F.J., Zhu J.Y. Exploration on the effectiveness and mechanism of CO2 carbonized slag-CaO-MgO reinforced soil. Journal of Geotechnical Engineering, 2019, 41 (12): 2197-2206.

[6] Wang D.X., Wang H.W., Zou W.L., et al. Study on durability of activated MgO-fly ash cured silt. Geotechnics, 2019, 40(12):4675-4684.DOI:10.16285/j.rsm.2018.1844.

[7] Zhong Y. Q., Cai G. H., Wang J. G., et al. Experimental study on the strength and conductivity characteristics of GGBS-activated MgO carbonized/stabilized zinc contaminated soil. Journal of Geotechnical Engineering, 2021, 43(S2):221-224.

[8] Chen J.H., He Y.Y., HU Yafeng. Mechanical property test of granulated blast furnace slag-magnesium oxide cured Lianyungang soft soil. Journal of Forestry Engineering, 2019, 4(02):133-138.DOI:10.13360/j.issn.2096-1359.2019.02.021.

[9] Ren K.B., Wang B., Li X.M., et al. Dry and wet cycle effects on mechanical properties of soil sites under low stress level. Journal of Rock Mechanics and Engineering, 2019, 38(02):376-385.DOI:10.13722/j.cnki.jrme.2018.0988.

[10] Kong X.H., Liang Y.P., Zhang J.G., et al. Experimental study on magnesium oxide-desulfurization gypsum-steel slag joint curing of dredged substrate. Journal of Chongqing Jiaotong University (Natural Science Edition), 2023, 42 (12): 61-69.

[11] Yi Y, Zheng X, Liu S, et al. Comparison of reactive magnesia-and carbide slag-activated ground granulated blastfurnace slag and Portland cement for stabilisation of a natural soil. Applied Clay Science, 2015, 111: 21-26.

